The Astrophysical Journal, 652:L000–L000, 2006 November 20

A POST-AGB STAR IN THE SMALL MAGELLANIC CLOUD OBSERVED WITH THE *SPITZER* INFRARED SPECTROGRAPH

Kathleen E. Kraemer,[1] G. C. Sloan,[2] J. Bernard-Salas,[2] Stephan D. Price,[1] Michael P. Egan,[1] and P. R. Wood[3]
Received 2006 June 23; accepted 2006 September 29; published 2006 October 23

ABSTRACT

We have observed an evolved star with a rare combination of spectral features, MSX SMC 029, in the Small Magellanic Cloud (SMC) using the low-resolution modules of the Infrared Spectrograph on the *Spitzer Space Telescope*. A cool dust continuum dominates the spectrum of MSX SMC 029. The spectrum also shows both emission from polycyclic aromatic hydrocarbons (PAHs) and absorption at 13.7 μm from C_2H_2, a juxtaposition seen in only two other sources, AFGL 2688 and IRAS 13416−6243, both post–asymptotic giant branch (AGB) objects. As in these sources, the PAH spectrum has the unusual trait that the peak emission in the 7–9 μm complex lies beyond 8.0 μm. In addition, the 8.6 μm feature has an intensity as strong as the C−C modes that normally peak between 7.7 and 7.9 μm. The relative flux of the feature at 11.3 μm to that at 8 μm suggests that the PAHs in MSX SMC 029 either have a low-ionization fraction or are largely unprocessed. The 13–16 μm wavelength region shows strong absorption features similar to those observed in the post-AGB objects AFGL 618 and SMP LMC 11. This broad absorption may arise from the same molecules that have been identified in those sources: C_2H_2, C_4H_2, HC_3N, and C_6H_6. The similarities between MSX SMC 029, AFGL 2688, and AFGL 618 lead us to conclude that MSX SMC 029 has evolved off the AGB in only the past few hundred years, making it the third post-AGB object identified in the SMC.

Subject headings: circumstellar matter — Magellanic Clouds — stars: AGB and post-AGB

1. INTRODUCTION

As a star ascends the asymptotic giant branch (AGB), its outer atmosphere expands and pulsates, pushing gas away from the star where it can cool and condense into dust grains. The resulting circumstellar dust shell hides the star in the optical and emits strongly in the infrared (IR). Eventually this mass-loss process will eject enough mass to expose the high-temperature core of the star, ionizing the gas inside the dust shell and forcing the transition from an AGB star to a planetary nebula. Objects making this transition are in their "post-AGB" phase (sometimes referred to as the "proto–planetary nebula" phase). Dust and gas characteristics change rapidly in this very short evolutionary stage, and the sources identified as post-AGB objects display a wide variety of properties. Van Winckel (2003) provides a good review of Galactic post-AGB objects and their general (albeit often disparate) properties. One of the challenges in understanding this phase of stellar evolution is identifying post-AGB candidates. Distinguishing post-AGB objects from other types of sources with circumstellar dust often depends on the derived luminosity for which a reliable distance is needed. While distances for field star candidates can be problematic, those for objects in the Large and Small Magellanic Clouds (LMC, SMC) are well constrained. Wood & Cohen (2001) identified 25 post-AGB candidates in the LMC using 8 μm data from the *Midcourse Space Experiment* (*MSX*) and near-IR *JK* observations. To date though, only two post-AGB objects have been identified in the SMC, IRAS 00350−7436 (Whitelock et al. 1989) and [KVS2000] MIR 1 (Kučinskas et al. 2000). Stellar evolution is also dependent on metallicity, but many of the details are not well understood. Thus, identification and observation of additional post-AGB objects in the LMC and SMC are therefore necessary for characterizing this phase of stellar evolution.

2. OBSERVATIONS AND DATA REDUCTION

We observed MSX SMC 029[4] with the Infrared Spectrograph (IRS; Houck et al. 2004) on the *Spitzer Space Telescope* (Werner et al. 2004) on 2004 October 25 as part of a project to study circumstellar dust shells in the SMC. The observations used the Short-Low (SL) and Long-Low (LL) modules, which have a wavelength range of 5–36 μm and an average spectral resolution of ~100. We extracted the spectra from the *Spitzer* Science Center S13.2 (SL) and S14.0 (LL) pipeline data. Near-IR observations were made from 2004 November 25 to 2005 September 19 at the Siding Spring Observatory (SSO) using the near-IR imaging system CASPIR (Cryogenic Array Spectrometer/Imager). MSX SMC 029 was detected only at *H* and *K* bands (the Two Micron All Sky Survey [2MASS] also detected it, J00364631−7331351, at *H* and *K* but not at *J*). The IRS and near-IR data reduction followed the standard procedures described in detail by Sloan et al. (2006). Table 1 gives the near-IR photometry from both the SSO and 2MASS. Figure 1 shows the IRS spectrum: MSX SMC 029 has a unique mid-IR spectrum, unlike any known Galactic or extragalactic object.

3. RESULTS AND DISCUSSION

3.1. *Evolutionary Status*

MSX SMC 029 shows the unusual combination of both C_2H_2 absorption at 13.7 μm and polycyclic aromatic hydrocarbon (PAH) emission features. In its spectral energy distribution (SED), F_ν peaks at ~17 μm, which corresponds to $T_d \approx 280$ K, although the SED is quite broad, so warmer and colder components are also present. We estimated the IR lu-

[1] US Air Force Research Laboratory, Space Vehicles Directorate, 29 Randolph Road, Hanscom AFB, MA 01731; kathleen.kraemer@hanscom.af.mil, steve.price@hanscom.af.mil, michael.egan@osd.mil.
[2] Department of Astronomy, Cornell University, 108 Space Sciences Building, Ithaca, NY 14853; sloan@isc.astro.cornell.edu, jbs@isc.astro.cornell.edu.
[3] Research School of Astronomy and Astrophysics, Mount Stromlo Observatory, Weston Creek, ACT 2611, Australia; wood@mso.anu.edu.au.

[4] We follow the nomenclature of Egan et al. (2001). In the *MSX* Point Source Catalog Ver. 2.3 (Egan et al. 2003), MSX SMC 029 = G304.3649−43.5610.

TABLE 1
NEAR-IR PHOTOMETRY OF MSX SMC 029

Date	*H*	*K*	Source
1998 Aug 08	15.75 ± 0.18	13.50 ± 0.04	2MASS
2004 Nov 25	15.79 ± 0.07	13.75 ± 0.17	SSO
2005 Jan 26	...	13.67 ± 0.06	SSO
2005 Mar 12	...	13.92 ± 0.08	SSO
2005 Jul 24	...	13.74 ± 0.03	SSO
2005 Sep 19	...	13.74 ± 0.05	SSO

NOTE.—*K*-band wavelengths are $K_s = 2.17$ μm for 2MASS and $K = 2.22$ μm for SSO

minosity L(1–100 μm) ~(4.5–5.5) × 10^3 $L_\odot$ by integrating the IRS spectrum and extrapolating longward of the IRS range with a 265 K graybody and shortward with a 530 K graybody, both scaled to match the IRS data. In order to determine its likely evolutionary state, we examined Galactic spectra (Kraemer et al. 2002; Sloan et al. 2003) from the Short Wavelength Spectrometer (SWS; de Graauw et al. 1996) on the *Infrared Space Observatory* (Kessler et al. 1996) and from IRS observations of LMC objects (Buchanan et al. 2006). As noted above, no other object has this combination of mid-IR SED and spectral features: warm dust, PAH emission, and C_2H_2 absorption. We therefore discuss the possible evolutionary phases that MSX SMC 029 could represent.

Pre–main sequence?—Strong PAH emission is commonly observed in H II regions and young stellar objects (YSOs), but C_2H_2 is not, particularly not at the strength observed in MSX SMC 029. Of the handful of YSOs in which weak C_2H_2 has been detected (e.g., Lahuis & van Dishoeck 2000 and references therein), only one has (very weak) PAH emission in its SWS spectrum. All have much colder SEDs than MSX SMC 029, peaking longward of the 45 μm SWS band edge, and have strong absorption from oxygen-rich silicates at 10 μm and often CO_2 at 15.5 μm. The luminosity of MSX SMC 029 is also much lower than the lowest luminosity H II regions identified in the LMC sample of Buchanan et al. (2006), which have L(1–100 μm) > 1.7 × 10^4 $L_\odot$. Most of the H II regions in the LMC sample show evidence of being extended, such as flux jumps 50% at 14 μm (between the SL and LL modules) or extended emission in the IR or visible images. MSX SMC 029 shows neither of these effects. It is unlikely, therefore, that MSX SMC 029 is either a YSO or an H II region.

Planetary nebula?—PAHs have also been observed in Galactic planetary nebulae (PNe), but again C_2H_2 absorption has not. Young PNe typically have dust temperatures of ~150 K. MSX SMC 029 does not have any emission from the highly ionized lines often observed in PNe. While the lack of ionized lines and warm dust does not strictly eliminate the PN possibility, the presence of C_2H_2 does.

AGB star?—Another possibility is that MSX SMC 029 is an evolved star but is still on the AGB. Carbon-rich AGB stars typically have C_2H_2 absorption at 13.7 μm, but they do not have PAH emission because they do not produce sufficiently hard radiation fields to excite PAHs. Furthermore, AGB stars with similar near-IR colors ($H - K \gtrsim 2$) in the LMC have *K*-band amplitudes of $\Delta K \sim 1.5$ mag (e.g., Wood 1998), much greater than the $\Delta K = 0.43$ mag observed in MSX SMC 029 (Table 1). The OGLE database (Szymański 2005) contains a star ~2.″2 from the 2MASS position with *I* magnitude ~19.2 but no variability above the noise. The presence of PAHs, together with the lack of strong *K*-band variability, implies that MSX SMC 029 cannot be an AGB star.

Post-AGB object?—Only two spectra in the SWS database show both PAH emission and C_2H_2 absorption at 13.7 μm, IRAS 13416−6243 and AFGL 2688 (the Cygnus Egg), both post-AGB sources. We examined all of the spectra from carbon-rich sources (groups 3, 4, and 5, subgroups CR, CT, CN, PU, U, and UE defined by Kraemer et al. 2002). On this basis alone, MSX SMC 029 looks to be a post-AGB object. No other possibility fits. In addition, as we show below, the PAH spectrum from MSX SMC 029 shows deviations from the standard PAH spectrum consistent with those seen in other post-AGB objects. AFGL 2688 is thought to be only a few hundred years past the AGB stage (Herpin et al. 2002). The dust around MSX SMC 029 is similar, significantly cooler than typically seen around AGB stars, so it is probably of a similar age. Because the dust around MSX SMC 029 is warmer than that around AFGL 2688, it may be even closer to the transition.

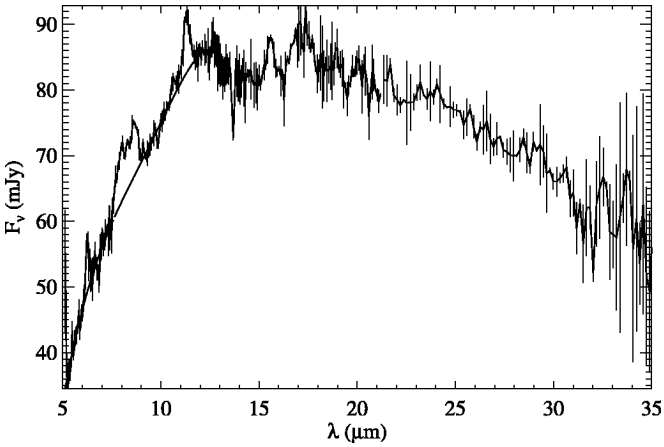

FIG. 1.—IRS spectrum of MSX SMC 029. Uncertainties reflect the differences between the two nods. The thin, smooth line from 5 to 13 μm shows the continuum level subtracted from the spectrum to extract the PAH features (see text).

3.2. *Solid-State Features*

To extract the PAH features for analysis, we fit a sixth-order polynomial to the spectrum between 5 and 13 μm (smooth line in Fig. 1). Figure 2 shows the "continuum"-subtracted result, and Table 2 contains the central wavelengths and fluxes of the detected features. Following Sloan et al. (2005), we extracted the PAH strengths by trapezoidal integration of the emission above a line fit to the continuum to either side using the wavelength ranges given in Table 2. The central wavelength λ_c is the wavelength at which half the integrated flux lies to the red and half to the blue. Table 2 also includes fluxes for the two components of the 7–9 μm feature complex. The flux at 12.7 μm is an upper limit; higher sensitivity data are needed to confirm this possible feature. Confident detection of a PAH feature at ~17 μm is precluded by the molecular absorption in the region (see § 3.3).

The most striking characteristic of the PAH features is their wavelength shift compared to more typical PAH spectra, as shown in Figure 3. Adopting the classification introduced by Peeters et al. (2002), the PAHs in MSX SMC 029 are class C, a category with only two sources from the SWS database, IRAS 13416 and AFGL 2688, and more recently, HD 233517, an O-rich AGB star with PAH emission from a circumstellar disk observed by the IRS (Jura et al. 2006). In those spectra, the 6.2 μm feature is shifted to 6.3 μm, and the peak of the 7–9 μm PAH complex, which usually occurs at 7.65 or 7.85 μm, is shifted to the red of 8.0 μm. In MSX SMC 029, these features are centered at 6.26 and 8.23 μm, respectively. Excluding the 8.6 μm C−H in-plane bend-

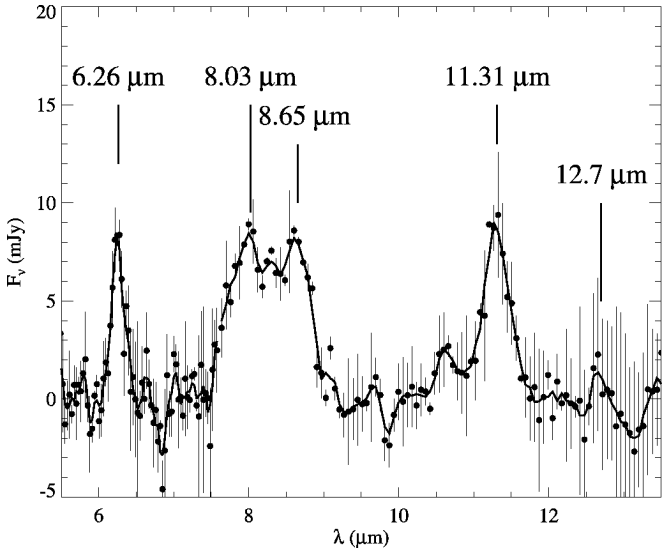

FIG. 2.—Continuum-subtracted PAH spectrum for MSX SMC 029. The data are the filled circles with error bars. The line shows the spectrum after smoothing with a 3 pixel boxcar. The labels indicate the central wavelengths of the PAH features. The 12.7 μm feature was only tentatively detected.

ing mode by fitting a line under it shifts the center from 8.23 to 8.12 μm. Alternatively, fitting Gaussians to the two components produces centers at 8.03 and 8.65 μm. However one measures it, the C−C modes usually seen at 7.65 and 7.85 μm here appear redward of 8.0 μm.

The positions and relative strengths of the PAH features have been attributed to the relative dominance of the ionization fraction of the PAHs, their composition, their isotopic ratios, their size, and the degree of UV processing they have undergone, to name a few. Vermeij et al. (2002), for example, examined the role of several of these factors in a small sample of LMC H II region spectra and suggested the molecular structure, which influences which C−C and C−H modes are present, may control the strengths in the LMC sources. Bregman & Temi (2005) found that the relative strengths of the 7.65 and 7.85 μm features in extended reflection nebulae vary, with the dominant emission shifting from 7.65 to 7.85 μm as the UV field grows weaker. Sloan et al. (2005) interpreted their PAH spectra from Herbig Ae/Be (HAeBe) stars similarly. These spectra are excited by weak UV fields, and the peak component in this region has shifted farther to the red, to 7.9–8.0 μm. The spectrum of MSX SMC 029 follows this trend, with the centroid of the C−C modes at 8.1–8.2 μm.

Other characteristics of the PAH spectrum from MSX SMC 029 are consistent with this shift in the C−C modes. The entire 7–9 μm PAH complex is only ~4 times stronger than the out-of-plane C−H bending mode at 11.3 μm, compared to 8–30 times stronger in the HAeBe stars (Sloan et al. 2005), indicating that the ionization fraction of the PAHs is lower in MSX SMC 029. Hony et al. (2001) studied the PAH features in the 11–13 μm region in 16 SWS spectra and found that the relative strengths of the solo and trio C−H out-of-plane bending modes at 11.3 and 12.7 μm varied with ionization fraction, with more ionized PAHs having a stronger trio mode at 12.7 μm. They interpreted this result as an indication of PAH processing, with more unprocessed PAHs having long, regular edges and thus more emission in the solo mode. In MSX SMC 029, the ratio of the 12.7 μm trio mode to the 11.3 μm solo mode is at most 0.25 (using the upper limit at 12.7 μm), as low as any in the

TABLE 2

PAH WAVELENGTHS AND FLUXES

λ_c (μm)	Flux (10^{-16} W m^{-2})	λ_{blue} (μm)	λ_{red} (μm)
6.26 ± 0.03	1.55 ± 0.27	5.80–5.95	6.65–6.80
8.23 ± 0.06	3.38 ± 0.24	7.30–7.60	9.00–9.30
11.32 ± 0.05	0.64 ± 0.10	10.80–11.05	11.85–11.95
12.69	<0.15	12.35–12.60	13.25–13.40
8.03	2.50	...	...
8.65	1.41	...	...

NOTE.—λ_{blue} and λ_{red} are the ranges over which the line segments were fit for the flux integration. Approximate fluxes for the components of the 7–9 μm complex are from integrating the Gaussian fits. Thus, the sum of the fluxes does not equal the total given for 8.23 μm.

sample examined by Hony et al. (2001). They also show that this ratio decreases as the ionization fraction decreases. The PAH spectrum of MSX SMC 029 follows this trend, indicating both a low-ionization fraction (low 7–9 μm/11.3 μm ratio) and relatively unprocessed PAHs (low 12.7 μm/11.3 μm ratio).

3.3. *Molecular Absorption Features*

Cernicharo et al. (2001) recently made the first detections of the polyacetylenic molecules C_4H_2 (diacetylene) and C_6H_2 outside the solar system in the very young post-AGB objects AFGL 618 and AFGL 2688, as well as detecting the more familiar

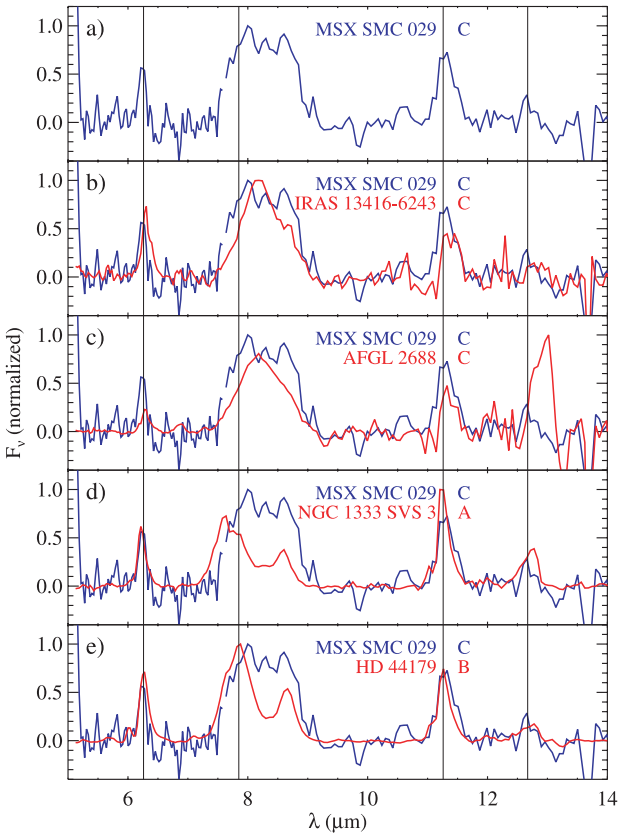

FIG. 3.—(*a*) 7–9 μm complexes from MSX SMC 029 (*blue line*) compared with (*red lines*) (*b*) the post-AGB object IRAS 13416−6243 (class C PAHs); (*c*) the post-AGB object AFGL 2688 (class C); (*d*) the young stellar object NGC 1333 SVS 3 (class A); and (*e*) the planetary nebula HD 44179 (class B). All the spectra have had the continuum approximated with a polynomial and subtracted. The spectral resolution of the SWS data was degraded to match that of IRS. The vertical lines are at the typical class B positions of 6.26, 7.85, 11.2, and 12.7 μm.

bands of C_2H_2 (acetylene) at 13.7 μm and HCN at 14 μm. In MSX SMC 029, the C_2H_2 band is the most prominent and easily identified molecular absorption feature. The limited signal-to-noise ratio and trouble determining a continuum level make extracting other features challenging. Fortunately, Bernard-Salas et al. (2006) recently observed the post-AGB object SMP LMC 11 with both the high- and low-resolution modules of IRS. They identified several hydrocarbons in the high-resolution spectrum whose fingerprints are also clearly discernible in the low-resolution spectrum. In addition to C_2H_2, their spectrum shows absorption from C_6H_6 and HC_3N (benzene and cyanoacetylene) at ~15 μm and C_4H_2 at ~16 μm. Figure 4 compares MSX SMC 029 to SMP LMC 11. The similarity of the spectra leads us to suggest that the same molecules may be shaping the MSX SMC 029 spectrum. The absorption near 16 μm in MSX SMC 029 has an additional red component that could be from C_6H_2 as was seen in AFGL 618 (Cernicharo et al. 2001). Absorption from the *P*- and *R*-branches of the C_2H_2 feature may affect the appearance of the spectra as well. The strong mid-IR absorption and nondetection at the *J* band, combined with a preliminary model that suggests high visual opacity, imply the presence of very dense material. This could be a residual circumstellar envelope from the AGB phase, which would be consistent with the youth of the post-AGB object, although such a nebula may require more extreme youth than is likely, or the material could be in the form of a dense disk.

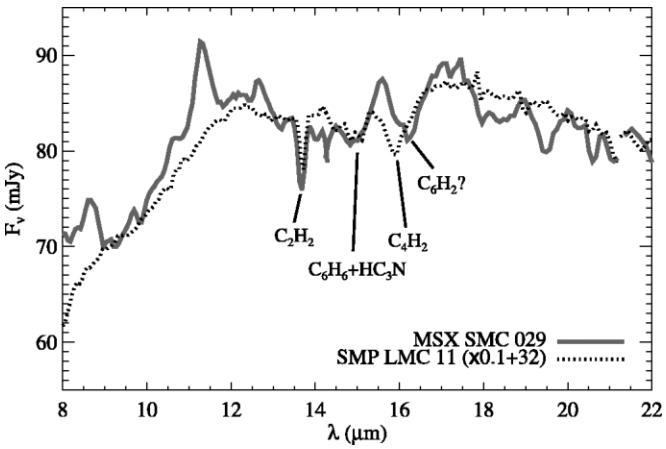

FIG. 4.—Comparison of MSX SMC 029 (*solid line*) with the IRS spectrum from the post-AGB object SMP LMC 11 (*dotted line*, scaled and offset to facilitate comparison). The molecular absorption features identified in the high-resolution spectrum of SMP LMC 11 (Bernard-Salas et al. 2006) and AFGL 2688 (Cernicharo et al. 2001) are indicated.

4. SUMMARY

We obtained a 5–35 μm low-resolution spectrum from MSX SMC 029 with the *Spitzer* IRS. It has an unusual spectral energy distribution and combination of mid-IR spectral features. MSX SMC 029, like the post-AGB objects AFGL 2688 and IRAS 13416−6243, shows both C_2H_2 absorption at 13.7 μm and PAH emission features. The PAHs in MSX SMC 029 are in the rare C class of Peeters et al. (2002). The shape of the 7–9 μm PAH complex and the relative flux of the 11.3 μm feature to that of the 12.7 μm feature suggest that MSX SMC 029 has a low-ionization fraction or unprocessed PAHs. The 13–16 μm wavelength region is similar to that of SMP LMC 11 and may be shaped by the same absorption features that have been resolved in the LMC source and in AFGL 618: C_2H_2, C_4H_2, HC_3N, C_6H_6, and possibly C_6H_2. We suggest that MSX SMC 029 is a very young post-AGB object, only the third known in the SMC.

We thank M. Matsuura for useful discussions on molecular absorption and color-color diagrams and the referee for helpful suggestions that improved the Letter. This work is based on observations made with the *Spitzer Space Telescope*, which is operated by JPL/Caltech under NASA contract 1407. Support for this work was provided in part by NASA through contract 1257184 (G. C. S. and J. B.-S.); P. R. W. received funding for this work from the Australian Research Council. This research has made use of NASA's Astrophysics Data System Bibliographic Services, data products from 2MASS, which is a joint project of the University of Massachusetts and IPAC/Caltech funded by NASA and the NSF, and the Simbad database operated at CDS, Strasbourg, France.

REFERENCES

Bernard-Salas, J., Peeters, E., Sloan, G. C., Cami, J., Guiles, S., & Houck, J. R. 2006, ApJ, 652, L000
Bregman, J., & Temi, P. 2005, ApJ, 621, 831
Buchanan, C. L., Kastner, J. H., Forrest, W. J., Hrivnak, B. J., Sahai, R., Egan, M., Frank, A., & Barnbaum, C. 2006, AJ, 132, 1890
Cernicharo, J., Heras, A. M., Tielens, A. G. G. M., Pardo, J. R., Herpin, F., Guélin, M., & Waters, L. B. F. M. 2001, ApJ, 546, L123
de Graauw, T., et al. 1996, A&A, 315, L49
Egan, M. P., van Dyk, S. D., & Price, S. D. 2001, AJ, 122, 1844
Egan, M. P., et al. 2003, Air Force Res. Lab. Tech. Rep. AFRL-VS-TR-2003-1589
Herpin, F., Goicoechea, J. R., Pardo, J. R., & Cernicharo, J. 2002, ApJ, 577, 961
Hony, S., Van Kerckhoven, C., Peeters, E., Tielens, A. G. G. M., Hudgins, D. M., & Allamandola, L. J. 2001, A&A, 370, 1030
Houck, J., et al. 2004, ApJS, 154, 18
Jura, M., et al. 2006, ApJ, 637, L45
Kessler, M. F., et al. 1996, A&A, 315, L27
Kraemer, K. E., Sloan, G. C., Price, S. D., & Walker, H. J. 2002, ApJS, 140, 389
Kučinskas, A, Vansevičius, V, Sauvage, M., & Tanabé, T. 2000, A&A, 353, L21
Lahuis, F., & van Dishoeck, E. F. 2000, A&A, 355, 699
Peeters, E., Hony, S., Van Kerckhoven, C., Tielens, A. G. G. M., Allamandola, T. L., Hudgins, D. M., & Bauschlicher, C. W. 2002, A&A, 390, 1089
Sloan, G. C., Kraemer, K. E., Matsuura, M., Wood, P. R., Price, S. D., & Egan, M. P. 2006, ApJ, 645, 1118
Sloan, G. C., Kraemer, K. E., Price, S. D., & Shipman, R. F. 2003, ApJS, 147, 379
Sloan, G. C., et al. 2005, ApJ, 632, 956
Szymański, M. 2005, Acta Astron., 55, 43
Van Winckel, H. 2003, ARA&A, 41, 391
Vermeij, R., Peeters, E., Tielens, A. G. G. M., & van der Hulst, J. M. 2002, A&A, 382, 1042
Werner, M., et al. 2004, ApJS, 154, 1
Whitelock, P. A., Feast, M. W., Menzies, J. W., & Catchpole, R. M. 1989, MNRAS, 238, 769
Wood, P. R. 1998, A&A, 338, 592
Wood, P. R., & Cohen, M. 2001, in Post-AGB Objects as a Phase of Stellar Evolution, ed. R. Szczerba & S. K. Górny (Dordrecht: Kluwer), 71